Biomedical Research (Tokyo) **37** (2) 141–151, 2016

Immunolocalization of osteocyte-derived molecules during bone fracture healing of mouse ribs

Zhusheng Liu[1], Tomomaya Yamamoto[1], Tomoka Hasegawa[1], Hiromi Hongo[1], Kanako Tsuboi[1], Erika Tsuchiya[1], Mai Haraguchi[1], Miki Abe[1], Paulo Henrique Luiz de Freitas[2], Akira Kudo[3], Kimimitsu Oda[4], Minqi Li[5], and Norio Amizuka[1]

[1] Department of Developmental Biology of Hard Tissue Graduate School of Dental Medicine, Hokkaido University, Sapporo, Japan; [2] Dental School, Federal University of Sergipe at Lagarto, Aracaju, Brazil; [3] Department of Biological Information, Tokyo Institute of Technology, Yokohama, Japan; [4] Division of Biochemistry, Niigata University Graduate School of Medical and Dental Sciences, Niigata, Japan; and [5] Shandong Provincial Key Laboratory of Oral Biomedicine, The School of Stomatology, Shandong University, Jinan, China

(Received 5 January 2016; and accepted 15 February 2016)

ABSTRACT

We employed a well-standardized murine rib fracture model to assess the distribution, in the cortical bone, of three important osteocyte-derived molecules—dentine matrix protein 1 (DMP1), sclerostin and fibroblast growth factor 23 (FGF 23). Two days after the fracture, the periosteum thickened, and up to the seventh day post-fracture, the cortical surfaces were promoting neoformation of two tissue types depending on the distance from the fracture site: chondrogenesis was taking place near the fracture, and osteogenesis distant from it. The cortical bones supporting chondrogenesis featured several empty lacunae, while in the ones underlying newly-formed woven bone, empty lacunae were hardly seen. DMP1-immunopositive osteocytic lacunae and canaliculi were seen both close and away from the fracture. In contrast, the region close to the fracture had only few sclerostin- and FGF23-immunoreactive osteocytes, whereas the distant region revealed many osteocytes immunopositive for these markers. Mature cortical bone encompassing the native cortical bone was observed at two-, three- and four-weeks post-fracture, and the distribution of DMP1, sclerostin and FGF23 appeared to have returned to normal. In summary, early stages of fracture healing seem to be important for triggering chondrogenesis and osteogenesis that may be regulated by osteocytes via their secretory molecules.

Fracture healing is a sequence of biological processes that include new formation of cartilage and bone. The tissue composed of newly-formed cartilage and bone, referred to as "callus", is the product of a coordinated physiological cascade that involves proliferation and differentiation of various lineages of inflammatory cells, angioblasts, fibroblasts, chondroblasts, and osteoblasts (24, 32). The initial cellular event is supposed to be cell replication of periosteal mesenchymal cells in the tissues surrounding the fracture site. After that, chondroblastic and osteoblastic differentiation ensues to promote the growth of a scaffold of cartilaginous and bony tissue, which is needed for initial bridging of the fracture gap. Through endochondral ossification, bone tissue gradually replaces the cartilaginous callus that was essential for primary stabilization of the fractured bone.

There are reports showing that periosteal mesenchymal cells respond to locally increased levels of growth factors and cytokines, and may differentiate into chondrocytes or osteoblasts (41), so that, the periosteal mesenchymal environment appears to influence such cell fate (4). In spite of the local ef-

Address correspondence to: Norio Amizuka, DDS, PhD
Department of Developmental Biology of Hard Tissue, Graduate School of Dental Medicine, Hokkaido University, Kita 13 Nishi 7 Kita-ku, Sapporo 060-8586, Japan
Tel: +81-11-706-4223, Fax: +81-11-706-4226
E-mail: amizuka@den.hokudai.ac.jp

fects of chondro-osteogenic factors, it is important to know whether the chondrocytic and osteoblastic precursors are derived from the same cell population, or whether they rise from one of two distinct periosteal layers: the outer "fibrous layer" and the inner "cambium layer", also referred to as the "osteoblastic layer". In a previous study, the cambium layer seemed to comprise the intrinsic periosteal component with respect to bone formation (5). Ito *et al.* demonstrated that the cambium layer, not the fibrous layer, serves as a reservoir of undifferentiated cells that are able to differentiate into osteoblasts and chondrocytes (15). Our previous study showed that, after cell proliferation had been stimulated in the cambium layer, cartilage and bone were regenerated having as source the native bone surfaces close to and distant from the fracture site (19).

In addition to the periosteal reaction, osteocytes might also have a role in the cascade of cellular events that ultimately lead to fracture healing. There is a common understanding that living osteocytes are mechanosensory cells that translate mechanical loading into cell signals, thereby regulating bone remodeling indirectly. Some ideas on how this may actually happen have been proposed, *e.g.,* stretch-activated ion channels (25), shear stress from interstitial fluid flow (8, 33) leading to the release of biochemical mediators such as nitric oxide and prostaglandins (1, 9, 14, 17, 43), and controlling of cell-to-cell communication via gap junctions (10). Therefore, it is likely that osteocytes influence periosteal osteoblasts in physiological and pathological circumstances, including bone fracture healing. Osteocyte-derived molecules were highlighted because the synthesis of these molecules may reflect osteocytic functions related to mechanosensing, regulation of bone remodeling and so forth. Many studies have reported on important osteocyte-derived factors, which regulate osteoblastic activities (sclerostin), affect proximal renal tubules to reduce serum concentrations of inorganic phosphorus (fibroblast growth factor 23, FGF23) and adhere to calcium phosphates in bone matrix (dentin matrix protein1, DMP1).

DMP1 is a bone matrix protein expressed by osteocytes that plays a supposedly important role in bone mineral homeostasis due to its high calcium-binding affinity (11, 35). Another osteocyte-derived factor, sclerostin, is a glycoprotein encoded by the *Sost* gene (40), and was reported to bind the LRP5/6 receptor—thereby antagonizing Wnt signaling and increasing β-catenin degradation (21, 37). Hence, sclerostin is known as a negative regulator of osteoblastic bone formation (27, 31, 36), as it is secreted by osteocytes, passes through the osteocytic canaliculi and inhibits the activation of bone-lining osteoblasts. On the other hand, there are reports on FGF23-driven modulation of adequate serum phosphate concentrations, which are required for normal skeletal development as well as preservation of bone integrity (28). Although FGF23 mRNA is found in several tissues (22, 30, 34), it is most abundantly expressed in bone (39). As a circulating factor secreted by osteocytes, FGF23 inhibits phosphate reabsorption and $1\alpha,25(OH)_2D_3$ production in the kidney (30), thereby acting on phosphate homeostasis. In addition, an *in vitro* study has demonstrated that overexpression of FGF23 resulted in the suppression on matrix mineralization (38). Thus, osteocytes may govern periosteal cells' response to fractures by controlling the secretion of molecules such as DMP1, sclerostin and FGF23.

In this study, we employed the mouse rib fracture model established by Li *et al.* (19) to examine the immunolocalization of osteocyte-derived molecules in an attempt to foster the understanding on the role of osteocytes in prompting chondrogenesis/osteogenesis in fractured bones.

MATERIALS AND METHODS

Animals and tissue preparation. All animal experiments in this study were conducted under the Hokkaido University Guidelines for Animal Experimentation (research proposal approved under No.11-0005). Thirty six male ICR mice at 8 weeks of age (weighing about 30 g; CLEA Japan Tokyo, Japan) were anesthetized with an intraperitoneal injection of 8% chloral hydrate (400 mg/100 g body weight). A transverse fracture was made with scissors on the right eighth rib of each mouse, as previously described (19). After the procedure, mice were housed with free access to water and to a powder diet. Antibiotics were not given to the operated mice. Animals were sacrificed at 2-, 4-, 7-days and 2-, 3- and 4-weeks after fracture creation ($n = 6$ for each). Mice were anesthetized as described above, and fixation was performed with a transcardiac perfusion of 4% paraformaldehyde in a 0.1 M phosphate buffer (pH 7.4). Following fixation, the eighth rib and surrounding muscles were removed *en bloc*, immersed in the same fixative for an additional 18 h and decalcified with 10% EDTA-2Na solution for 4 weeks at 4°C. After demineralization, the specimens were dehydrated through an ascending ethanol series prior to paraffin embedding.

Immunohistochemistry for DMP1, sclerostin, FGF23, periostin and tissue nonspecific alkaline phosphatase. Dewaxed sections were treated with 0.1% hydrogen peroxide for 15 min. After pre-incubation with 1% bovine serum albumin (BSA; Serologicals Proteins Inc., Kankakee, IL) in PBS (1% BSA-PBS) for 30 min at room temperature (RT), the serial histological sections were incubated with rabbit antibody against DMP1 (Takara Bio Inc., Otsu, Japan) at a dilution of 1 : 300, with rabbit polyclonal antisera against tissue nonspecific alkaline phosphatase (ALP) (26) at a dilution of 1 : 500 or with rabbit antibody to mouse periostin (14, 18) at a dilution of 1 : 500 with 1% BSA-PBS at RT. These sections were reacted with horseradish peroxidase (HRP)-conjugated goat anti-rabbit IgG (DakoCytomation, Glostrup, Denmark), proceeded rinsing with PBS. For detection of FGF23 and sclerostin, the dewaxed paraffin sections were treated with rat anti-FGF23 (R&D systems Inc., Minneapolis, MN) diluted at 1 : 100 for 2 h, or with goat anti-mouse sclerostin antibody (R&D systems) at a dilution of 1 : 100 for 2 h. Sections treated with the primary antibodies were subsequently incubated in HRP-conjugated anti-rat IgG (Chemicon International Inc., Temecula, CA) or HRP-conjugated anti-goat IgGs (Rockland Immunochemicals Inc., Gilbertsville, PA) at a dilution of 1 : 100 at RT. All immune complexes were visualized using 3,3'-diaminobenzidine tetrahydrochloride (DAB; Dojindo Laboratories, Kumamoto, Japan). All sections were counterstained with methyl green, and observed under a light microscope (Eclipse E800; Nikon Instruments Inc., Tokyo, Japan).

Quantification of the percentage of DMP1-, sclerostin- or FGF23-positive osteocytes. The cortical bone was divided into two areas: the area close to the fracture site (from the fracture surface to a putative, vertical line 500 μm distant from the facture) and the area distant from the fracture site (between two putative vertical lines 500 μm and 1000 μm distant from the fracture surface). Regarding the ratio of empty lacunae and lacunae with osteocytes, we counted the number of empty lacunae or lacunae including osteocytes in the regions close and distant from the fracture, and divided them by the total number of osteocytic lacunae, expressing the results in percentage ($n = 6$ for each).

For the percentages of DMP1-, sclerostin- and FGF23-positive osteocytes in cortical bone, we counted the numbers of DMP1-, sclerostin- or FGF23-positive osteocytes and then divided the counts by the numbers of living osteocytes in the regions close and distant from the fracture site ($n = 6$ for each). All values are presented as means ± standard deviation. Differences among groups were assessed by unpaired Student's *t*-test, and considered statistically significant when $P < 0.05$.

RESULTS

We have divided all experimental periods of fracture healing in two groups: early stage (2-, 4- and 7-days post-operation) and late stage (2-, 3- and 4-weeks post-operation). The early stage of fracture healing showed chondrogenesis/osteogenesis derived from the cortical surface, while the late stage displayed endochondral ossification.

Histological alteration of periosteum and cortical bones at post-fracture days 2, 4 and 7

After 2 days, the fracture line was smooth, and there was no evidence of inflammation in the surrounding tissues (Fig. 1A). The periosteum of the fractured rib was thickened and with high cellular density (Fig. 1B). Although ALP immunoreactivity, which is a hallmark of osteoblastic cells, was broadly seen in the thickened periosteum (Fig. 1C), periostin immunoreactivity still remained in the fibrous layer of periosteum, but in part, sparse throughout the periosteum (Fig. 1D). The cortical bone near the fracture site, henceforth referred to as "close region", showed several empty osteocytic lacunae, while higher counts of intact osteocytes were found in the region distant from the fracture site, or "distant region" (Fig. 1B). At post-fracture day 4, two different, but intertwined matrices faintly stained with hematoxyline or eosin seemed to derive from the native periosteal surface of the close and the distant regions, respectively (Fig. 1E, F). In serial sections, ALP- and periostin-immunoreactivity was weakened to be sparse in such matrices (Fig. 1G, H). At post-fracture day 7, cartilaginous matrices had arisen from the periosteal surfaces of the close region, while woven bone had formed at the distant region neighboring the cartilaginous matrix (Fig. 1I, J). Many chondrocytes and osteocytes were embedded in the newly formed cartilage and bone, respectively (Fig. 1J). Interestingly, several osteocytic lacunae were empty beneath the close region, where chondrogenesis was taking place; on the other hand, living osteocytes were present in the distant region, from which woven bone was arising. ALP-immunoreactivity was seen associated with newly-formed woven bone, while periostin was distributed mainly in the outer regions of the cartilage and woven bone (Fig. 1K, L).

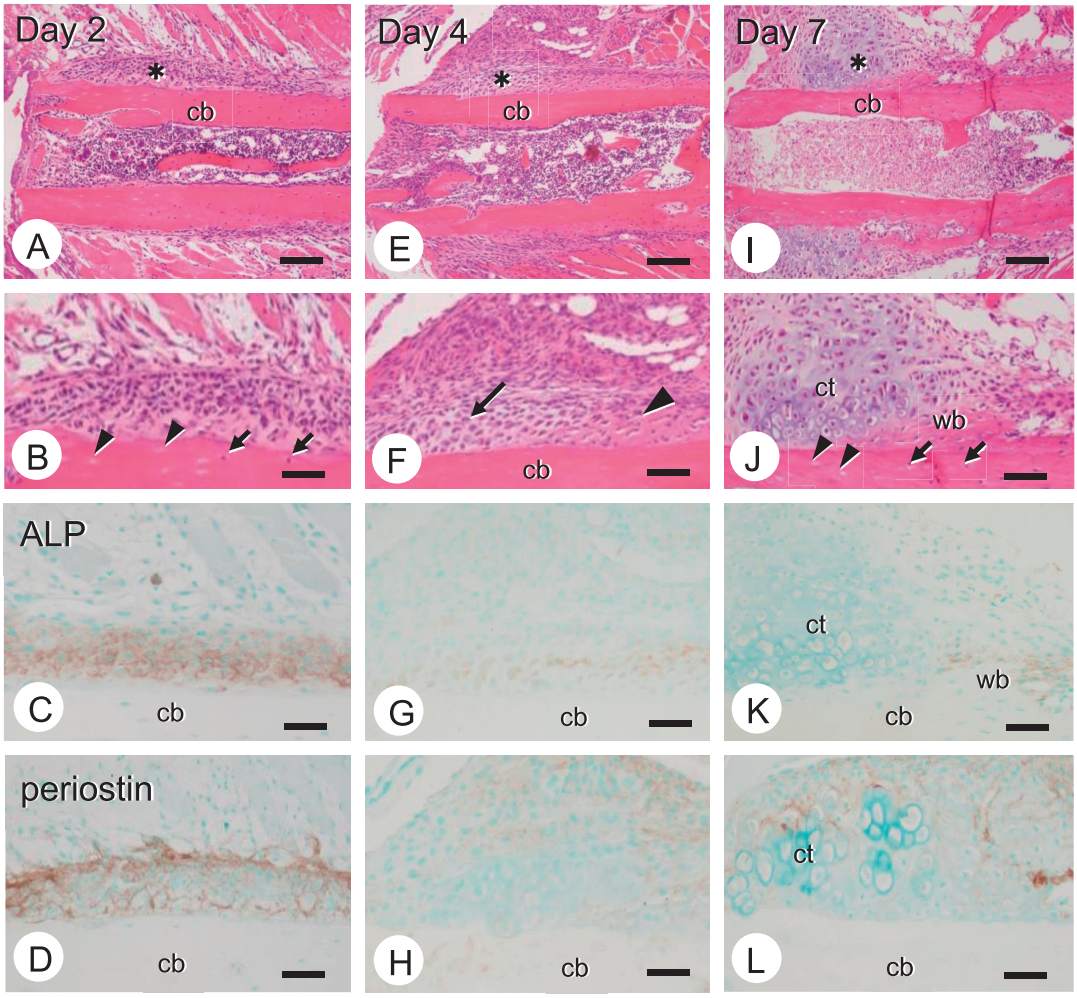

Fig. 1 Histology of periosteum and cortical bones at days 2, 4 and 7. Panels **A**–**D**, **E**–**H** and **I**–**L** represent histology and immunohistochemistry for ALP and periostin at days 2, 4, and 7. After 2 days of the fracture, the periosteum of the fractured rib was thickened (an asterisk in **A**). At a higher magnification, the thickened periosteum is shown to have a high cellular density (**B**), and reveals the broad immunoreactivity for ALP (brown color, **C**) and overlying periostin (brown color, **D**). Notice empty lacunae (arrowheads) and lacunae with osteocytes (arrows) in panel **B**. At day 4 (**E**, **F**), the thickened periosteum shows two different neighboring matrices faintly stained with hematoxyline (an arrow in **F**) or eosin (an arrowhead, **F**). Note that the former and latter matrices derive from the native periosteal surface of the close and the distant regions. Weak ALP-immunoreactivity is seen in some cells in the thickened periosteum (faint brown color, **G**), while periostin is sparsely observed throughout the matrix (**H**). At day 7 (**I**, **J**), apparent cartilaginous matrices (ct) and woven bone (wb) are developed from the close and distant regions of the cortical bones (cb), neighboring each other (**J**). Note that there are empty lacunae (arrowheads, **J**) beneath the newly-formed cartilage, while osteocytes (arrows, **J**) can be seen in the distant region, from which woven bone is arising. ALP-immunoreactivity is associated with newly-formed woven bone (**K**), and periostin is sparsely distributed (**L**). Bars, A, E, I: 100 μm, B–D, F–H, J–L: 50 μm

Immunolocalization of DMP1, sclerostin and FGF23 in the cortical bones at post-fracture day 2

Empty lacunae were found mainly in the close region, whereas living osteocytes were seen in the distant region in the early stages of fracture healing. The ratio of empty lacunae/lacunae occupied with osteocytes was 87.52 vs 12.48 in the close region and 18.14 vs 81.86 in the distant region at post-fracture day 2 (Fig. 2G). In the close region, the majority of osteocytic lacunae and canaliculi were positive for DMP1 (Fig. 2A), but little sclerostin- and FGF23-immunopositivity was identified (Fig. 2C, E), when compared with those in the distant region (Fig. 2B, D, F). Statistical analyses demonstrated significantly higher indices of sclerostin- and FGF23-reactive osteocytes in the distant region compared to those in the close region (Fig. 2H). There was no significant difference in the index of DMP1-positive osteocytes

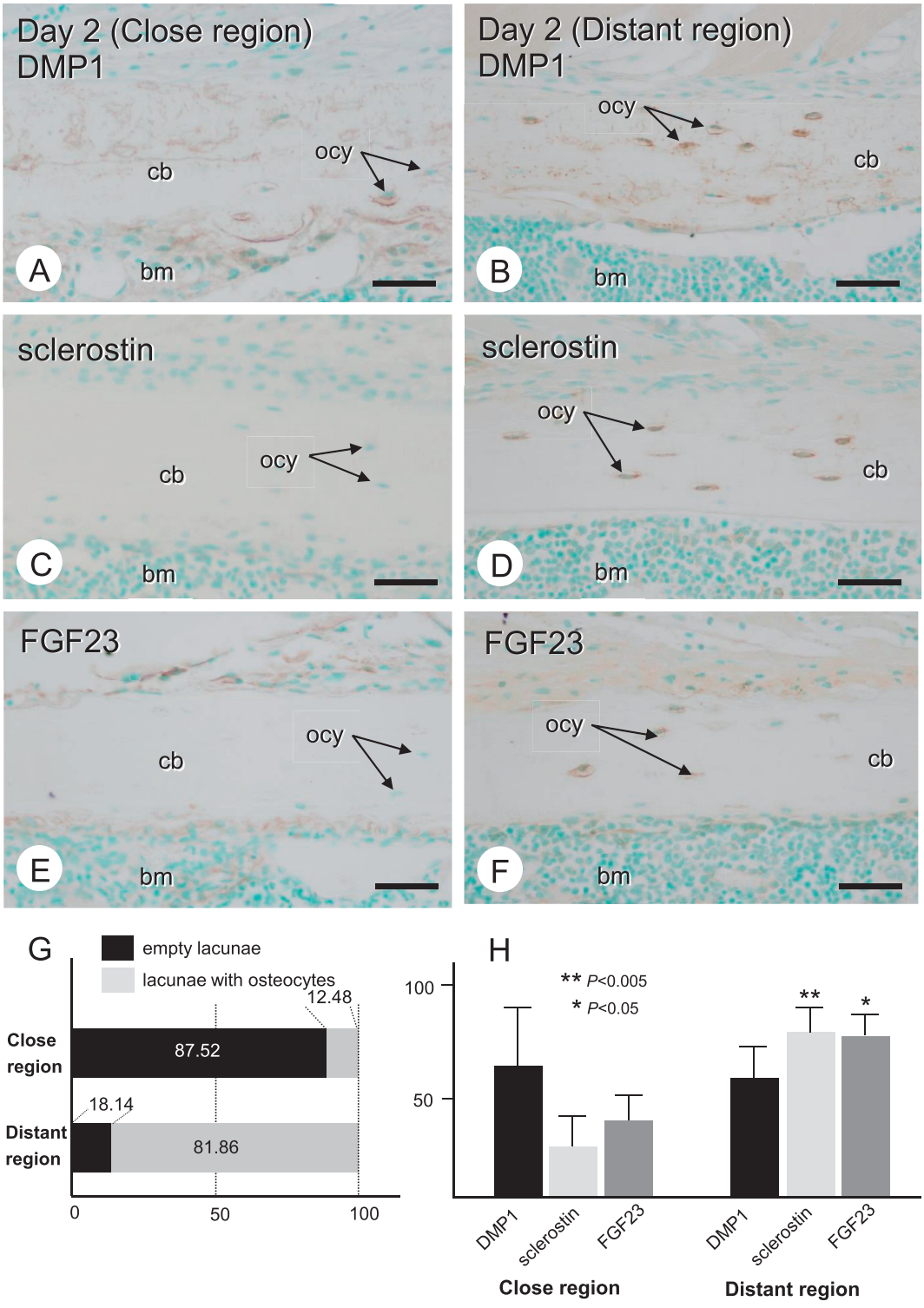

Fig. 2 Immunolocalization of DMP1, sclerostin and FGF23 in the cortical bones at day 2. Panels **A**, **C** and **E** derive from the cortical bone (**cb**) close to the fracture site, while panels **B**, **D** and **F** are the cortical bones distant from the fracture site. Although there are only a few osteocytes (ocy) in the close regions (**A**, **C**, **E**), the distant regions show many DMP1 (**B**)-, sclerostin (**D**)- and FGF23 (**F**)-immunopositive osteocytes (ocy). Panel **G** reveals the ratio of empty lacunae/lacunae occupied with osteocytes. Panel **H** is a statistical analysis for evaluating the percentage of DMP1-, sclerostin- and FGF23-positive osteocytes divided by the number of intact osteocytes. Note significantly higher indices of sclerostin- and FGF23-reactive osteocytes in the distant region compared to those in the close region. bm: bone marrow. Bars, A–F: 50 μm

(Fig. 2H).

Immunolocalization of DMP1, sclerostin and FGF23 in the cortical bones at post-fracture day 4

The ratio of empty lacunae/lacunae occupied with osteocytes was 87.04 vs 12.96 in the close region and 18.97 vs 81.03 in the distant region at post-fracture day 4 (Fig. 3G). As seen at post-fracture day 2, most osteocytic lacunae and canaliculi were positive for DMP1 in the close and in the distant regions (Fig. 3A, B). In contrast, the close region had few sclerostin- and FGF23-immunopositive osteocytes while the distant region exhibited many osteocytes positive for those two proteins (Fig. 3C–F). Statistical analyses verified the significantly higher counts of sclerostin- and FGF23-immunopositive osteocytes in the distant region, without a clear change in the distribution of DMP1 (Fig. 3H). The main difference from the previous stage was the presence of fibroblast-like cells showing a faint immunoreactivity for FGF23, which were found in bone marrow near the fracture site (See an inset of Fig. 3E).

Immunolocalization of DMP1, sclerostin and FGF23 in the cortical bones post-fracture day 7

The ratio of empty lacunae/lacunae occupied with osteocytes did not dynamically change at day 7 compared to earlier stages (77.01 vs 22.99 in the close region and 11.69 vs 88.31 in the distant region) (Fig. 4G). The close region showed abundant DMP1-positive osteocytic lacunae (Fig. 4A) and few sclerostin- and FGF23-reactive osteocytes (Fig. 4C, E), whereas osteocytes in the distant region were reactive for DMP1, sclerostin and FGF23 (Fig. 4B, D, F). Several fibroblastic cells in the bone marrow near the facture site still showed intense FGF23 reactivity (Fig. 4E).

Histological alteration and immunolocalization of sclerostin and FGF23 in the cortical bones at post-fracture week 2, 3 and 4

In the later stages, cartilage associated with the native cortical bone underwent endochondral ossification (Fig. 5). Cartilage and woven bone were evident at post-fracture week 2 and 3 (Fig. 5A, B, D, E). As endochondral ossification proceeded, an outer newly-formed cortical bone was gradually growing and covering the inner native cortical bone by week 4 (Fig. 5C, F). This outer cortical bone was thick and mature, with less cartilage remnants.

Sclerostin-immunopositivity was all evident in most osteocytes in the newly-formed outer cortex and in the native inner cortical bone (Fig. 5G–I). Although FGF23-immunoreactivity was present in fibroblastic cells from the bone marrow and in the granulation tissues surrounding the fracture after 2 and 3 weeks (Fig. 5J, K), the population of non-osteocytic FGF23-positive cells reduced gradually as endochondral ossification proceeded (Fig. 5L).

DISCUSSION

It is important to understand how periosteal cells and osteocytes interact in the circumstance of fracture healing. To our knowledge, this is the first report to demonstrate the chronological distribution of osteocyte-derived molecules—DMP1, sclerostin and FGF23—as chondrogenesis and osteogenesis progressed. In this study, the early stages of fracture healing (up to post-fracture day 7) seem essential for determining the sites at which chondrogenesis or osteogenesis would take place.

A previous study of ours, which employed the same animal model used here, clearly demonstrated stimulated cell proliferation in the cambium layer as the initial cellular event in fracture healing (19). Our studies have confirmed that chondrogenesis and osteogenesis occur having the periosteal surfaces in regions close and distant from the fracture site as their foundation, suggesting that the cambium cell layer is capable of chondrogenic and osteogenic differentiation. This is in agreement with reports by Ito *et al.*, which described that osteoblasts in the cambium layer remain in a bipotential state as "preosteochondrocytes" (15, 16).

Bone fractures destroy osteocytes and sever the meshwork of osteocytic cytoplasmic processes, and empty osteocytic lacunae appeared in the cortical bone consequent to the fracture. Curiously, healing initially came in the form of chondrogenesis near the fracture site, where osteocytic lacunae were empty. On the other hand, osteogenesis took place in the region where osteocytes were alive and occupied their lacunae. In addition to the increased ratio of the empty lacunae, the indices of sclerostin/FGF23-immunopositive osteocytes, however, imply that several living osteocytes did not synthesize sclerostin and FGF23 near the fracture site. It is possible that the blockade of osteocyte-derived factors such as sclerostin and FGF23 affects the function and differentiation of periosteal osteoblasts, since osteocytes and osteoblasts are coupled via gap junctions that can transmit a variety of stimuli (10).

Another interesting finding in this work is the unusual localization of FGF23. After the fracture, osteocytes near the fracture site ceased synthesizing

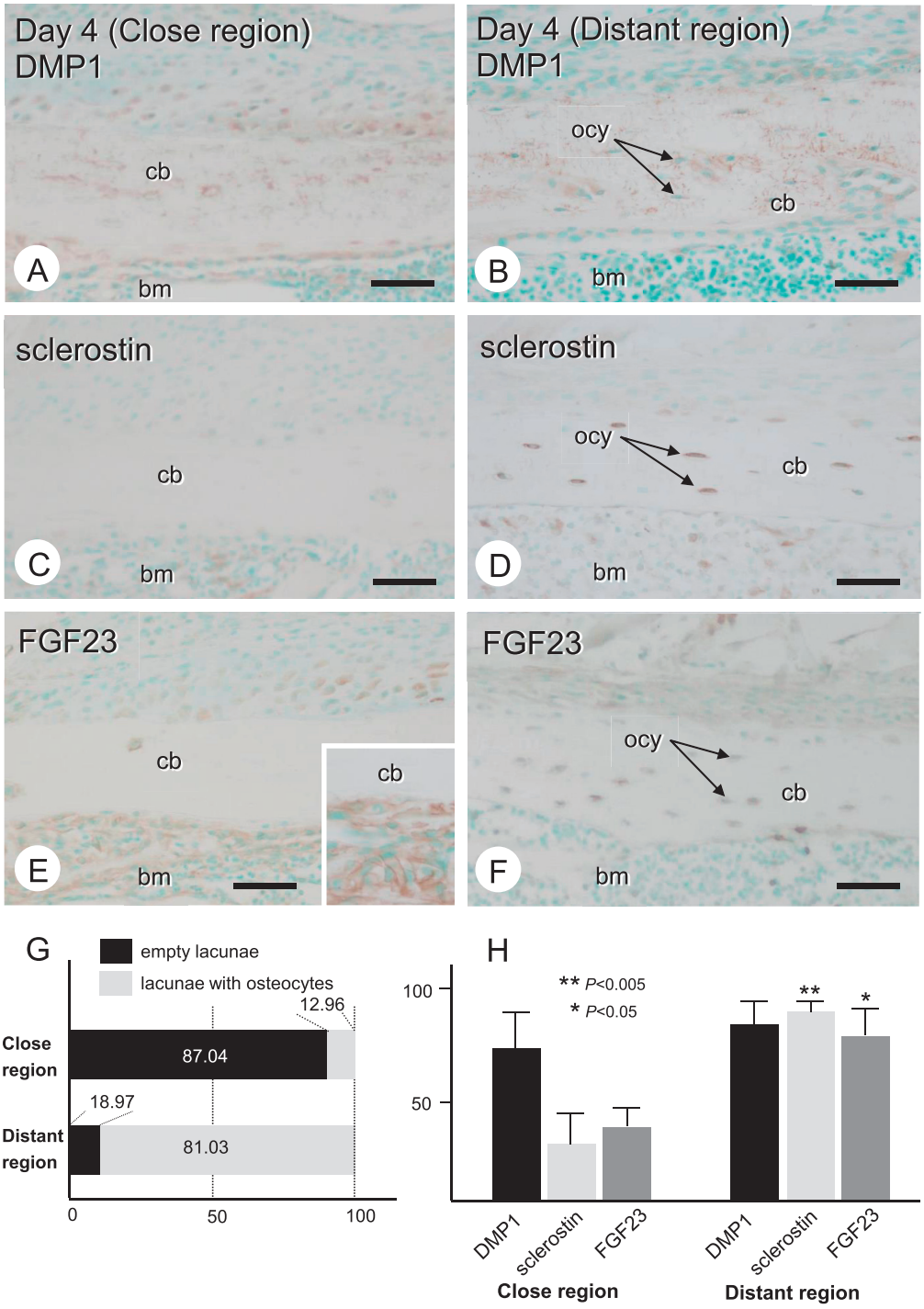

Fig. 3 Immunolocalization of DMP1, sclerostin and FGF23 in the cortical bones at day 4. Panels **A**, **C** and **E** represent the cortical bones (cb) close to the fracture site, whereas panels **B**, **D** and **F** show the cortical bones distant from the fracture site. The periosteal region shows a high cellularlity, and the underlying cortical bones have empty lacunae (**A**, **C**, **E**). There is few sclerostin (**C**)- and FGF23 (**E**)-positive osteocytes in the close regions, while DMP1-positive lacunae can be seen (**A**). Notice FGF23-immunoreactive fibroblastic cells in the region of bone marrow (an inset of panel **E**). In contrast, the distant regions demonstrate many DMP1 (**B**)-, sclerostin (**D**)- and FGF23 (**F**)-immunopositive osteocytes (ocy). The ratio of empty lacunae/lacunae occupied with osteocytes is shown in panel **G**. Statistical analyses demonstrate the indices of DMP1-, sclerostin- and FGF23-positive osteocytes between the close and distant regions. There are significantly higher indices of sclerostin- and FGF23-reactive osteocytes in the distant region compared to those in the close region. bm: bone marrow. Bars, A–F: 50 μm

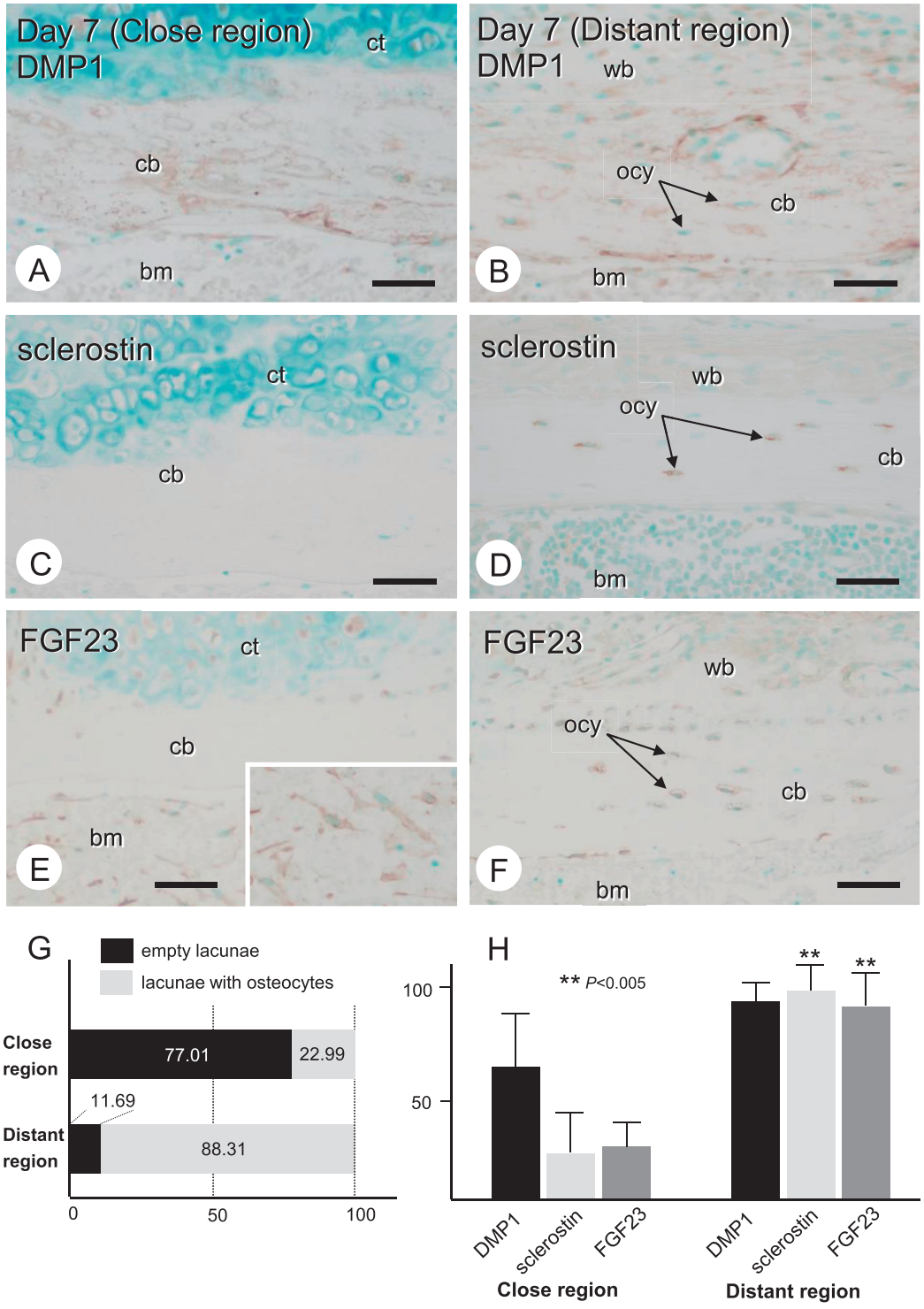

Fig. 4 Immunolocalization of DMP1, sclerostin and FGF23 in the cortical bones at day 7. Panels **A**, **C** and **E** are the cortical bone (cb) with newly-formed cartilage (ct) close to the fracture site, while panels **B**, **D** and **F** are the cortical bones with woven bones distant from the fracture site. The ratio of empty lacunae/lacunae occupied with osteocytes does not dynamically change at day 7 compared to earlier stages (**G**). The close region shows abundant DMP1-positive osteocytic lacunae (**A**) and few sclerostin (**C**)- and FGF23 (**E**)-reactive osteocytes. In contrast, osteocytes (ocy) in the distant region are immunoreactive for DMP1 (**B**), sclerostin (**D**) and FGF23 (**F**). Several fibroblastic cells in the bone marrow near the facture site still show FGF23 reactivity (**E**). Note significantly higher indices of sclerostin- and FGF23-reactive osteocytes in the distant region compared to those in the close region (**H**). bm: bone marrow. Bars, A–F: 50 μm

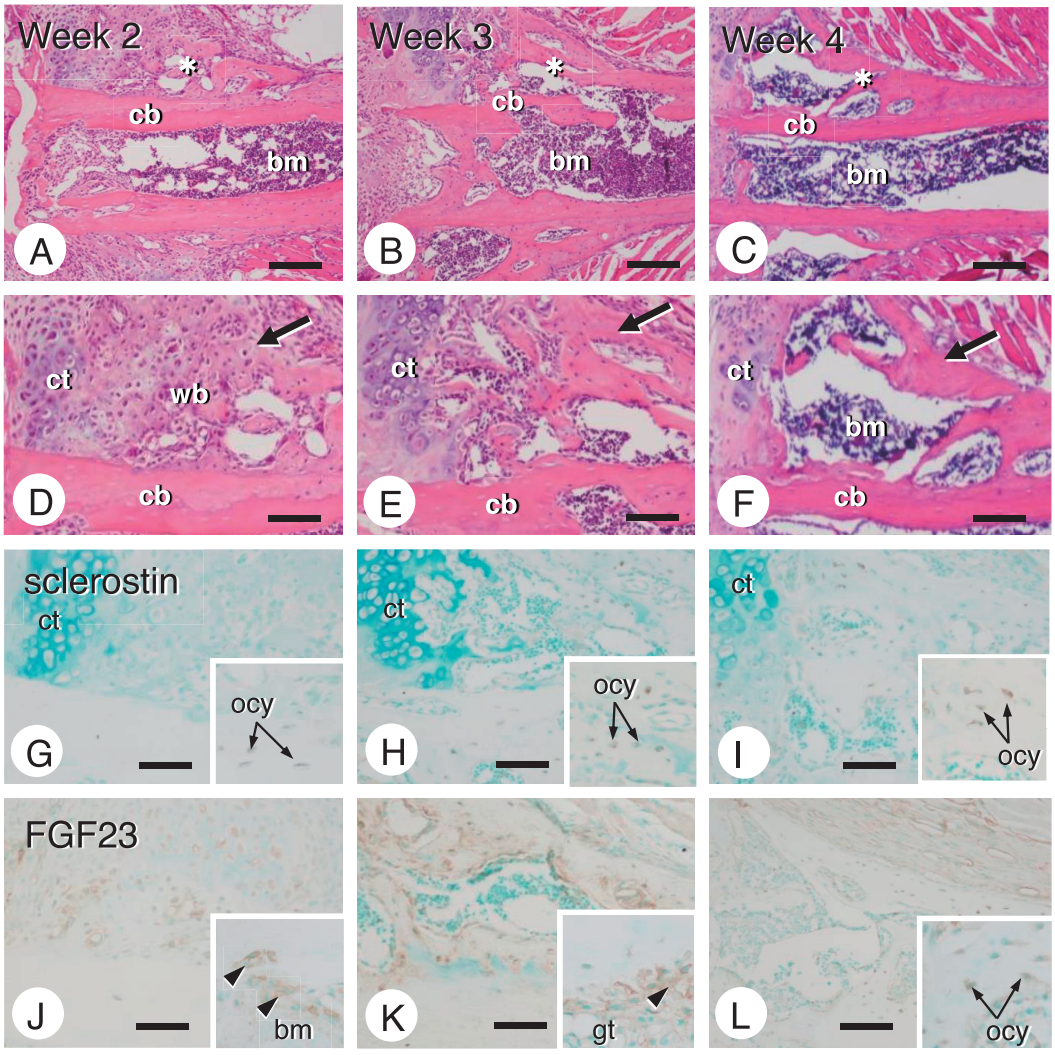

Fig. 5 Histological alteration and immunolocalization of sclerostin and FGF23 in the cortical bones at post-fracture weeks 2, 3 and 4. Cartilage (ct) and woven bone (wb) are evident at post-fracture week 2 (**A**, **D**). However, as time goes on, an outer newly-formed cortical bone (asterisks in **B** and **C**, arrows in **E** and **F**) becomes thick, covering the inner native cortical bone (cb in **B** and **C**) at weeks 3 and 4 (**B**, **C**, **E**, **F**). Sclerostin-immunoreactivity is observable in most osteocytes (ocy) in the newly-formed outer cortex and in the native inner cortical bone (See insets of **G**–**I**). FGF23-immunoreactive fibroblastic cells in the bone marrow (bm) and in the granulation tissues (gt) are prominent at weeks 2 and 3 (arrowheads in **J** and **K**), but cannot be observable at week 4 (**L**). Bars, A–C: 150 μm, D–L: 75 μm

FGF23; instead, fibroblastic cells in the bone marrow became FGF23-positive as early as post-fracture day 4, remaining so throughout post-fracture week 3. Goebel *et al.* have reported that FGF23 was synthesized in the granulation tissues surrounding bone fracture sites, suggesting that FGF23 is a possible parameter for bone healing (12). In our study, FGF23-producing fibroblastic cells were seen early in the bone marrow, and were still present in the granulation tissue 3 weeks after the fracture. As mentioned above, the early stages up to day 7 appear to be intrinsic for determining chondrogenesis or osteogenesis associated with cortical bones. Therefore, even though FGF23 affects osteogenic differentiation to some extent (38), the chronological changes in the localization of FGF23-synthesizing cells suggest that it does not serve as a determinant of chondrogenesis/osteogenesis. Nevertheless, it is possible that FGF23 acts locally in a way other than promoting chondrogenesis/osteogenesis, especially considering its role as regulator of inorganic phosphorus in serum (22, 28, 30, 34, 39).

Chondrogenesis and subsequent chondrocytic proliferation and differentiation are regulated by Wnt/

β-catenin signaling (2, 3, 6, 20, 42, 44). The cessation of sclerostin synthesis by osteocytes near the fracture site may lift the inhibition of Wnt/β-catenin signaling in periosteal cells, consequently inducing chondrogenesis. However, there are reports suggesting that Wnt/β-catenin signaling does not promote chondrogenesis (13, 29); it is well known that sclerostin inhibits osteoblast activity via Wnt/β-catenin signaling. Therefore, it does not also seem that Wnt/β-catenin signaling is a determinant of chondrogenesis/osteogenesis. Several authors share the notion that the cell surface receptor subtype to prostaglandin E2 (EP2) mediates the effects of autocrined prostaglandin E2 on the osteocytes' gap junction in response to fluid flow-induced shear stress (9, 17). In addition, EP2, cAMP, PKA and cyclooxygenase-2 are critical components of the signaling cascade that involves mechanical strain and gap junction-mediated communication among osteocytes (1, 7). Altogether, it seems likely that sclerostin and other factors affect periosteal differentiation, but the details of such effect and the nature of the factors involved is still unknown. Nevertheless, we found it rather intriguing that sclerostin synthesis, or the lack thereof, seemed to correlate spatially with either osteogenesis or chondrogenesis.

The precise function of osteocytes is still the subject of ongoing and fruitful scientific discussion. With the aid of molecular biology strategies, further studies will help unveiling the functions, the products and the effect of these cells on bone fracture healing.

Acknowledgments

This study was partially supported by the National Nature Science Foundation of China (Li M), Specialized Research Fund for the Doctoral Program of Higher Education (Li M), Grants-in Aid for Scientific Research (Amizuka N, Hasegawa T) and Promoting International Joint Research (Bilateral Collaborations) of JSPS and NSFC (Amizuka N, Li M).

REFERENCES

1. Ajubi NE, Klein-Nulend J, Alblas MJ, Burger EH and Nijweide PJ (1999) Signal transduction pathways involved in fluid flow-induced PGE2 production by cultured osteocytes. *Am J Physiol* **276**, E171–178.
2. Andrade AC, Nilsson O, Barnes KM and Baron J (2007) Wnt gene expression in the post-natal growth plate: regulation with chondrocyte differentiation. *Bone* **40**, 1361–1369.
3. Bradley EW and Drissi MH (2011) Wnt5b regulates mesenchymal cell aggregation and chondrocyte differentiation through the planar cell polarity pathway. *J Cell Physiol* **226**, 1683–1693.
4. Caplan AI (1987) Bone development of repair. *Bioassay* **6**, 171–175.
5. Carter DC and Giori NJ (1991) Effects of mechanical stress on tissue differentiation in the bony implant bed. In: *The Bone-material Interface*. (Davis JE ed), pp367–379, University of Toronto Press.
6. Chen M, Zhu M, Awad H, Li TF, Sheu TJ, Boyce BF, Chen D and O'Keefe RJ (2008) Inhibition of beta-catenin signaling causes defects in postnatal cartilage development. *J Cell Sci* **121**, 1455–1465.
7. Cheng B, Kato Y, Zhao S, Luo J, Sprague E, Bonewald LF and Jiang JX (2001) PGE(2) is essential for gap junction-mediated intercellular communication between osteocyte-like MLO-Y4 cells in response to mechanical strain. *Endocrinology* **142**, 3464–3473.
8. Cheng B, Zhao S, Luo J, Sprague E, Bonewald LF and Jiang JX (2001) Expression of functional gap junctions and regulation by fluid flow in osteocyte-like MLO-Y4 cells. *J Bone Miner Res* **16**, 249–259.
9. Cherian PP, Cheng B, Gu S, Sprague E, Bonewald LF and Jiang JX (2003) Effects of mechanical strain on the function of Gap junctions in osteocytes are mediated through the prostaglandin EP2 receptor. *J Biol Chem* **278**, 43146–43156.
10. Doty SB (1981) Morphological evidence of gap junctions between bone cells. *Calcif Tissue Int* **33**, 509–512.
11. George A, Gui J, Jenkins NA, Gilbert DJ, Copeland NG and Veis A (1994) In situ localization and chromosomal mapping of the AG1 (Dmp1) gene. *J Histochem Cytochem* **42**, 1527–1531.
12. Goebel S, Lienau J, Rammoser U, Seefried L, Wintgens KF, Seufert J, Duda G, Jakob F and Ebert R (2009) FGF23 is a putative marker for bone healing and regeneration. *J Orthop Res* **27**, 1141–1146.
13. Hill TP, Später D, Taketo MM, Birchmeier W and Hartmann C (2005) Canonical Wnt/beta-catenin signaling prevents osteoblasts from differentiating into chondrocytes. *Dev Cell* **8**, 727–738.
14. Horiuchi K, Amizuka N, Takeshita S, Takamatsu H, Katsuura M, Ozawa H, Toyama Y, Bonewald LF and Kudo A (1999) Identification and characterization of a novel protein, periostin, with restricted expression to periosteum and periodontal ligament and increased expression by transforming growth factor beta. *J Bone Miner Res* **14**, 1239–1249.
15. Ito Y, Fitzsimmons JS, Sanyal A, Mello MA, Mukherjee N and O'Driscoll SW (2001) Localization of chondrocyte precursors in periosteum. *Osteoarthritis Cartilage* **9**, 215–223.
16. Ito Y, Sanyal A, Fitzsimmons JS, Mello MA and O'Driscoll SW (2001) Histomorphological and proliferative characterization of developing periosteal neochondrocytes in vitro. *J Orthop Res* **19**, 405–413.
17. Jiang JX and Cheng B (2001) Mechanical stimulation of gap junctions in bone osteocytes is mediated by prostaglandin E2. *Cell Commun Adhes* **8**, 283–288.
18. Kii I, Amizuka N, Minqi L, Kitajima S, Saga Y and Kudo A (2006) Periostin is an extracellular matrix protein required for eruption of incisors in mice. *Biochem Biophys Res Commun* **342**, 766–772.
19. Li M, Amizuka N, Oda K, Tokunaga K, Ito T, Takeuchi K, Takagi R and Maeda T (2004) Histochemical evidence of the initial chondrogenesis and osteogenesis in the periosteum of a rib fractured model: implications of osteocyte involvement in periosteal chondrogenesis. *Microsc Res Tech* **64**, 330–342.
20. Li X, Peng J, Wu M, Ye H, Zheng C, Wu G, Xu H, Chen X and Liu X (2011) BMP2 promotes chondrocyte proliferation

via the Wnt/β-catenin signaling pathway. *Mol Med Rep* **4**, 621–626.
21. Li X, Zhang Y, Kang H, Liu W, Liu P, Zhang J, Harris SE and Wu D (2005) Sclerostin binds to LRP5/6 and antagonizes canonical Wnt signaling. *J Biol Chem* **280**, 19883–19887.
22. Liu S, Guo R, Simpson LG, Xiao ZS, Burnham CE and Quarles LD (2003) Regulation of fibroblastic growth factor 23 expression but not degradation by PHEX. *J Biol Chem* **278**, 37419–37426.
23. Liu S, Gupta A and Quarles LD (2007) Emerging role of fibroblast growth factor 23 in a bone-kidney axis regulating systemic phosphate homeostasis and extracellular matrix mineralization. *Curr Opin Nephrol Hypertens* **16**, 329–335.
24. Mckibbin B (1978) The biology of fracture healing in long bones. *J Bone Joint Surg Br* **60-B**, 150–162.
25. Mikuni-Takagaki Y (1999) Mechanical responses and signal transduction pathways in stretched osteocytes. *J Bone Miner Metab* **17**, 57–60.
26. Oda K, Amaya Y, Fukushi-Irie M, Kinameri Y, Ohsuye K, Kubota I, Fujimura S and Kobayashi J (1999) A general method for rapid purification of soluble versions of glycosylphosphatidylinositol-anchored proteins expressed in insect cells: An application for human tissue-nonspecific alkaline phosphatase. *J Biochem* **126**, 694–699.
27. Poole KE, van Bezooijen RL, Loveridge N, Hamersma H, Papapoulos SE, Löwik CW and Reeve J (2005) Sclerostin is a delayed secreted product of osteocytes that inhibits bone formation. *FASEB J* **19**, 1842–1844.
28. Quarles LD (2003) Evidence for a bone–kidney axis regulating phosphate homeostasis. *J Clin Invest* **112**, 642–646.
29. Roudier M, Li X, Niu QT, Pacheco E, Pretorius JK, Graham K, Yoon BR, Gong J, Warmington K, Ke HZ, Black RA, Hulme J and Babij P (2013) Sclerostin is expressed in articular cartilage but loss or inhibition does not affect cartilage remodeling during aging or following mechanical injury. *Arthritis Rheum* **65**, 721–731.
30. Shimada T, Mizutani S, Muto T, Yoneya T, Hino R, Takeda S, Takeuchi Y, Fujita T, Fukumoto S and Yamashita T (2001) Cloning and characterization of FGF23 as a causative factor of tumor-induced osteomalacia. *Proc Natl Acad Sci USA* **98**, 5945–5946.
31. Silvestrini G, Ballanti P, Leopizzi M, Sebastiani M, Berni S, Di Vito M and Bonucci E (2007) Effects of intermittent parathyroid hormone (PTH) administration on SOST mRNA and protein in rat bone. *J Mol Histol* **38**, 261–269.
32. Simmons DJ (1985) Fracture healing perspectives. *Clin Orthop* **200**, 100–113.
33. Srinivasan S and Gross TS (2000) Canalicular fluid flow induced by bending of a long bone. *Med Eng Phys* **22**, 127–133.
34. The ADHR Consortium (2000) Autosomal dominant hypophosphataemic rickets is associated with mutations in FGF23. *Nat Genet* **26**, 345–348.
35. Toyosawa S, Shintani S, Fujiwara T, Ooshima T, Sato A, Ijuhin N and Komori T (2001) Dentin matrix protein 1 is predominantly expressed in chicken and rat osteocytes but not in osteoblasts. *J Bone Miner Res* **16**, 2017–2026.
36. Van Bezooijen RL, Roelen BA, Visser A, van der Wee-Pals L, de Wilt E, Karperien M, Hamersma H, Papapoulos SE, ten Dijke P and Löwik CW (2004) Sclerostin is an osteocyte-expressed negative regulator of bone formation, but not a classical BMP antagonist. *J Exp Med* **199**, 805–814.
37. Veverka V, Henry AJ, Slocombe PM, Ventom A, Mulloy B, Muskett FW, Muzylak M, Greenslade K, Moore A, Zhang L, Gong J, Qian X, Paszty C, Taylor RJ, Robinson MK and Carr MD (2009) Characterization of the structural features and interactions of sclerostin: molecular insight into a key regulator of Wnt-mediated bone formation. *J Biol Chem* **284**, 10890–10900.
38. Wang H, Yoshiko Y, Yamamoto R, Minamizaki T, Kozai K, Tanne K, Aubin JE and Maeda N (2008) Overexpression of fibroblast growth factor 23 suppresses osteoblast differentiation and matrix mineralization in vitro. *J Bone Miner Res* **23**, 939–948.
39. Weber TJ, Liu S, Indridason OS and Quarles LD (2003) Serum FGF23 levels in normal and disordered phosphorus homeostasis. *J Bone Miner Res* **18**, 1227–1234.
40. Winkler DG, Sutherland MK, Geoghegan JC, Yu C, Hayes T, Skonier JE, Shpektor D, Jonas M, Kovacevich BR, Staehling-Hampton K, Appleby M, Brunkow ME and Latham JA (2003) Osteocyte control of bone formation via sclerostin, a novel BMP antagonist. *EMBO J* **22**, 6267–6276.
41. Yasui N, Sato M, Ochi T, Kimura T, Kawahata H, Kitamura Y and Nomura S (1997) Three modes of ossification during distraction osteogenesis in the rat. *J Bone Joint Surg Br* **79**, 824–830.
42. Yates KE, Shortkroff S and Reish RG (2005) Wnt influence on chondrocyte differentiation and cartilage function. *DNA Cell Biol* **24**, 446–457.
43. Zaman G, Pitsillides AA, Rawlinson SC, Suswillo RF, Mosley JR, Cheng MZ, Platts LA, Hukkanen M, Polak JM and Lanyon LE (1999) Mechanical strain stimulates nitric oxide production by rapid activation of endothelial nitric oxide synthase in osteocytes. *J Bone Miner Res* **14**, 1123–1131.
44. Zhu M, Chen M, Zuscik M, Wu Q, Wang YJ, Rosier RN, O'Keefe RJ and Chen D (2008) Inhibition of beta-catenin signaling in articular chondrocytes results in articular cartilage destruction. *Arthritis Rheum* **58**, 2053–2064.